Experience from using 3D CSEM in the Mexican deepwater exploration program

José Antonio Escalera Alcocer, Marco Vázquez García, and Humberto Salazar Soto, PEMEX Subdirección de Exploración; Friedrich Roth, Daniel Baltar, Pål T. Gabrielsen, and Valente Ricoy Paramo, EMGS*

Summary

PEMEX has acquired more than 9500 km^2 of wide-azimuth 3D controlled-source electromagnetic (CSEM) data as part of its deep water exploration program since 2010. The acquisition campaign is carried out systematically on a portfolio level and is designed to provide resistivity imaging on both prospect and regional scale. We present four examples of integrated interpretation with 3D seismic, demonstrating the information that can be extracted from the 3D CSEM data and applications of this information. The first example focuses on prospect maturation, where a resistivity anomaly is used as a direct hydrocarbon indicator (DHI). We discuss how evaluation of anomaly characteristics, such as correlation to seismic attributes, and field size estimation based on the area and strength of the anomaly can influence a prospect's probability of economic success. In the second example, we study potential drilling hazards and show how CSEM can help to identify gas hydrate variability in terms of thickness and concentration over a bottom simulating reflector (BSR). The third example relates to petroleum system analysis where CSEM inversion results are used to study the composition of diapirs, i.e. salt versus shale, and identify fluid migration pathways resulting from faulting. The last example describes regional mapping of resistivity, which may indicate variations in lithology, identify potential shallow hazards and even generate new leads. The cases we present exemplify the value of using CSEM systematically in a large frontier exploration program.

Introduction

The use of marine CSEM for hydrocarbon exploration started in 2000 with the successful field trial over the Girassol prospect, offshore Angola (Ellingsrud et al., 2002). The new exploration method was met by enormous industry interest, leading to the acquisition of a large number of calibration and exploration surveys in all major oil provinces around the world in the years following the successful Angola trial.

The first application of marine CSEM in Mexico goes back to early 2008, when a small number of 2D surveys was acquired in different exploration areas in the deepwater Gulf of Mexico. The results of these first surveys very much resemble the Statoil experience described in Buland et al. (2011): The surveys tended to be inconclusive due to the inadequacy of 2D surveys to handle complex geology, immature processing and imaging products, and lack of integrated interpretation and exploration workflows that use the CSEM information. Since then, the technology has matured significantly. Wide-azimuth 3D CSEM acquisition in combination with anisotropic 3D inversion (Zach et al., 2008) has become routine practice. This development has been supported by improvements in source and receiver equipment as well as vessel operations that allow for efficient acquisition of high quality electromagnetic data over large areas. In addition, oil companies that want to use the technology have become aware that they need to develop integrated workflows for prospect maturation, risking and resource estimation in order to extract full value from the CSEM data.

In 2010, PEMEX started an ambitious multi-year CSEM acquisition campaign as part of its deepwater exploration program. More than 9500 km^2 of wide-azimuth 3D CSEM data have been acquired since then. The CSEM strategy is to use the technology systematically on a portfolio level to be able to rank prospects for a particular play based on their seismic and CSEM expressions in combination with petroleum system analysis. The CSEM campaign mostly targets clastic turbidite deposits down to 3000 m depth below seabed in mid-slope to basin floor settings at water depths between 1000-3000 m. In addition to prospect maturation, the CSEM campaign also aims to provide information for an improved regional geology understanding in underexplored frontier areas where no well data exists. The regional approach also provides a platform for possible play and new lead identification.

The prospect oriented and regional goals of the CSEM campaign are met by a survey design based on rolling receiver grids (Fig. 1). Each grid typically consists of 120-130 seabed receivers measuring horizontal electric and

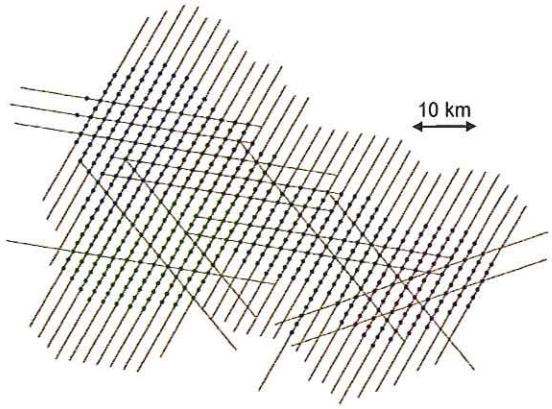

Figure 1: Typical survey design based on rolling grids.

DOI http://dx.doi.org/10.1190/segam2012-1181.1

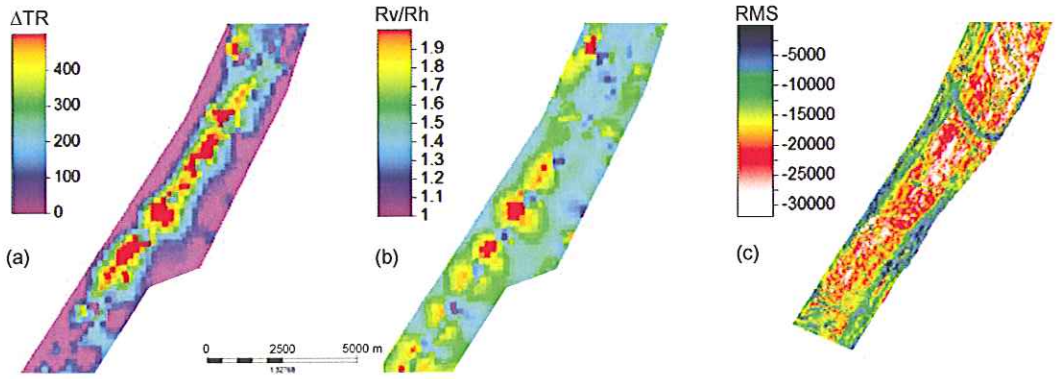

Figure 2: Analysis of a CSEM anomaly. (a) Anomalous transverse resistance; (b) electrical anisotropy; (c) seismic RMS amplitude.

magnetic field components. A receiver spacing of 1.5 km in-line and 2 km cross-line is used. The denser in-line spacing benefits the illumination of thin resistive layers and is usually chosen along the regional strike direction. The source towing and receiver operations are planned such as to provide a good balance between achieving uniform illumination across receiver grid boundaries and operational efficiency. Some crossing towlines are added for improved target delineation and background resistivity reconstruction.

In this abstract, we will share four data examples to illustrate the value of the information the CSEM campaign provides. The examples focus on integrated interpretation of anisotropic 3D CSEM inversion results with seismic. Each example describes a different application: prospect maturation, gas hydrate characterization, study of diapirism and identification of fluid migration paths, and regional resistivity mapping.

Prospect Maturation

Due to the strong sensitivity of formation resistivity to hydrocarbon saturation, CSEM is a very good direct hydrocarbon indicator (DHI). In practice, a good way to identify potentially hydrocarbon charged formations from 3D CSEM data is to represent the 3D inversion result as maps describing the cumulative resistivity measurement over a depth interval of interest. Such representation facilitates correlation with seismic surface attributes and is a natural choice given the relatively large vertical measurement scale of CSEM compared to seismic. In addition, even anomalies with low resistivity contrast may be revealed due to spatial coherence.

Figure 2 illustrates a typical integrated analysis based on resistivity maps for a small area from one of our surveys. The map on the left-hand side (Fig. 2a) plots the anomalous transverse resistance, i.e. the contrast in vertical resistivity multiplied by the thickness of the interval of interest, from which a clear CSEM anomaly can be identified. As in seismic DHI analysis, it is important to establish that the most likely cause of this anomaly is trapped hydrocarbons. This requires a detailed analysis of anomaly characteristics, including correlation to seismic data and geological models, and evaluation of possible interpretation pitfalls in the context of the regional setting. In combination with the evaluation of data quality metrics, such integrated analysis can be used to update the probability Pg of discovering a flowable hydrocarbon accumulation. The anomaly of Fig. 2 has a number of encouraging characteristics: Significant apparent electrical anisotropy (Fig. 2b), conformance to structure and good spatial correlation with RMS amplitude computed over a reflection interval consistent with the possible depth origin of the anomaly (Fig. 2c).

An important property of CSEM is that the strength of the measured response depends on the volume of resistive reservoir rock, i.e. area multiplied by net pay. In CSEM favorable environments, this volume sensitivity can result in a significant uncertainty reduction in the resource estimation since prospect area and net pay are typically associated with the highest uncertainties (P10/P90 ratios) in exploration. Baltar and Roth (2012) describe a method for computing a field size distribution (FSD) from the anomalous transverse resistance (Fig. 2a). The application of this method to our campaign has demonstrated the possibility to yield distributions with P10/P90 ratios in the range of 5-10. Observation of a CSEM anomaly tends to truncate the FSD on the lower end, thus favoring the presence of larger field sizes. Given a strong and large anomaly, the P90 estimate of recoverable resources may increase multifold. In contrast, observation of no CSEM anomaly tends to truncate the higher end of the FSD, i.e. it sets an upper limit to the largest field size supported by the CSEM data. Both cases are very relevant for deepwater exploration. Together with Pg, this information can be used to either increase or decrease a prospect's probability of economic success.

DOI http://dx.doi.org/10.1190/segam2012-1181.1

Gas Hydrate Characterization

Gas hydrates can pose a significant deepwater drilling risk. In seismic data, the presence of hydrates is typically inferred indirectly through observation of a bottom simulating reflector (BSR) associated with a velocity contrast due to free gas underneath the gas hydrate stability zone (GHSZ). Gas hydrates may therefore be difficult to identify under conditions where no clear velocity contrast occurs at the base of the GHSZ. Even when a BSR is observed, the hydrate thickness and the concentration often remain uncertain. In such cases, the resistivity information from CSEM provides useful complementary information for hydrate characterization, as the example below will show.

Figure 3 shows a shallow depth section of vertical resistivity extracted from a 3D CSEM inversion result and overlaid to the corresponding seismic depth section. The seismic data exhibits a BSR across the two structures shown, i.e. a "soft" reflection identified by a negative amplitude event (white) that follows the seabed topography. At the small anticline (left-hand side in Fig. 3), where older sediments have been uplifted by folding and faulting into the interpreted GHSZ, the seismic also seems to image the top of the hydrate accumulation by a "hard" positive amplitude event (black). This observation suggests a high acoustic velocity for the hydrate bearing sediments. Boswell et al. (2009) report a similar case in the Gulf of Mexico validated by well data, where both the top and the base of the hydrate interval are imaged by the seismic. In contrast, the younger sediments in the GHSZ of the main structure (right-hand side in Fig. 3) exhibit a transparent seismic expression. From the seismic data alone, it is difficult to say whether the transparency is caused by different sensitivity of the acoustic properties to the presence of hydrates, lower hydrate saturation, a thinner hydrate interval, or a combination of these factors. However, when integrated with the CSEM inversion result, the combined observations favor the interpretation that the hydrate thickness and saturation is non-uniform across the two structures. A strong resistivity anomaly with high transverse resistance is reconstructed at the small anticline, supporting the presence of a thick porous sandy interval with high hydrate saturation consistent with the seismic expression. Where the hydrates occur in the younger sediments, no significant resistivity anomaly is observed despite the high CSEM sensitivity at small depth, thus supporting an interpretation that conditions are less favorable for the accumulation of a thick high saturation hydrate package at the main structure.

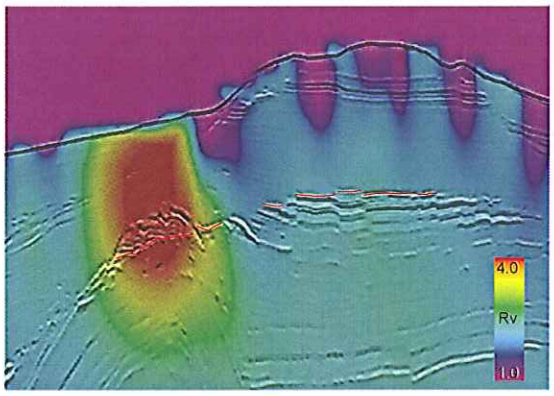

Figure 3: Shallow depth section of vertical resistivity along a BSR (red pick) indicating gas hydrate variability in terms of thickness and concentration.

Study of Diapirism

Diapirs, both salt and shale cored, create good potential for hydrocarbon accumulation. They tend to produce excellent traps through deformation of surrounding sediments and also as a result of their own impermeability to hydrocarbons. Faulting associated with diapiric development may also facilitate hydrocarbon migration. Despite these similarities, distinction between salt and shale diapirs is important for petroleum system analysis. For instance, the shale itself may be a source rock, i.e. there can be a direct causal relationship between shale diapirism and hydrocarbon accumulations. Moreover, the difference in heat conductivity and the association with different mother layers, in particular the usual tendency of shale diapirs to not intrude upwards from great depth, have significant consequences for the thermal history and the dynamics of a potential petroleum system.

In frontier exploration, establishing the nature of diapirism can be challenging, e.g. in transition zones between salt and shale dominated areas. Very pointy and near vertical diapir geometries can be challenging imaging targets for seismic, as a result of which salt diapir images may lack the "hard" reflection signature characteristic for salt. Since both salt and shale diapirs constitute low density contrasts compared to the surrounding sediments, distinction based on gravity data is often ambiguous. In such settings, CSEM data can provide an important piece of the puzzle due to the high resistivity property of salt.

Figure 4 shows a co-visualization of the vertical resistivity from 3D CSEM inversion and the seismic image of a diapir interpreted as salt. There are a number of indicators supporting this interpretation. To begin with, the top salt is associated with a "hard" reflection identified by a positive amplitude event (white). Furthermore, the diapir has been reconstructed by the CSEM inversion as having high resistivity. The diapir has an apparent electrical anisotropy factor less than one, which is a robust characteristic for a narrow vertical resistive structure. Most interestingly, the sediments above the diapir are very conductive. Looking closer at the seismic, the conductive zone is characterized by faulting, suggesting vertical migration of water with

DOI http://dx.doi.org/10.1190/segam2012-1181.1

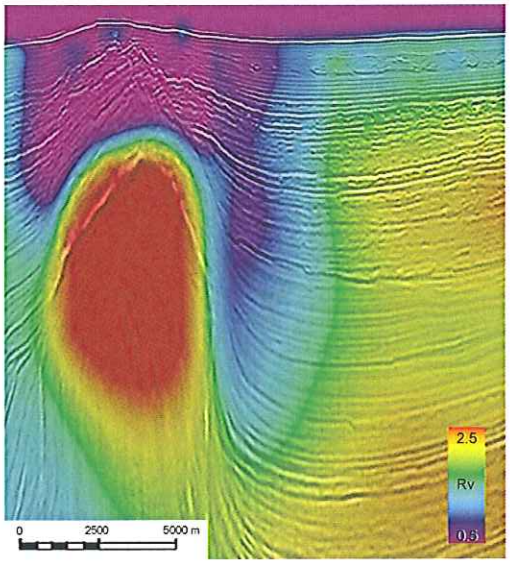

Figure 4: CSEM and seismic expression of a salt diapir. The conductive zone above the diapir has been interpreted as faults providing migration pathways for high salinity water.

abnormally high salinity. A possible explanation for the high salinity may be salt dissolution in connection with water expulsion from the sediment deformation. Once these salt indicators from seismic and CSEM had been established, they were used regionally as a template for analyzing the likelihood of a diapir being salt versus shale dominated.

Regional Resistivity Mapping

The survey design based on rolling receiver grids allows for generating resistivity maps for specific formations that indicate regional scale resistivity variations. Figure 5a shows an example map of vertical resistivity exhibiting a number of interesting features. The most noticeable features are conductive zones (blue), which in fact are expressions of fluid migration associated with faulting, as discussed in the previous section. Furthermore, a general trend of increasing resistivity from bottom to top is observed, which may indicate different lithofacies. Superimposed to this trend are more localized areas of high resistivity (red), in particular in the center-right part of the map. Prior to the CSEM acquisition, analysis of seismic amplitudes had been conducted in some parts of the study area and had indicated the possible presence of shallow gas, i.e. a drilling hazard. The regional resistivity image suggests the possibility of an alternative interpretation for the larger anomalies, i.e. as stratigraphic leads. Revisiting the seismic has shown expressions of channelized lobe systems supporting this idea (Fig. 5b). Of course this does not rule out that the anomalies have their origin in lithology or diagenesis, and more work is required to enhance the understanding of these potential leads.

Conclusions

Modern oil and gas exploration is driven by the integration of geophysics and geology. The presented data and interpretation examples demonstrate how 3D CSEM contributes to this integration and helps solving complex exploration challenges: direct hydrocarbon identification for prospect risking and resource estimation, gas hydrate detection and characterization for the evaluation of potential drilling hazards, study of diapirism for petroleum system analysis, identification of fluid migration pathways or, conversely, sealing of faults. Acquisition of wide-azimuth 3D CSEM data over large areas may also help to improve regional understanding and generate leads.

CSEM is still a fairly young technology, meaning that there are no ready-made solutions for these CSEM applications. To capture the value of CSEM, it is therefore essential to integrate CSEM into the common exploration workflows. It is equally important to recognize and address CSEM specific challenges and limitations. Examples that we have encountered during our CSEM campaign are low sensitivity as a result of low resistivity pay, ambiguity in reconstructing target depth and in resolving stacked objectives due to the limited vertical resolution, and imaging challenges for prospects in the proximity of salt or in rough bathymetric terrain. Finally, it is important to establish an experience database containing careful analysis of the CSEM results against drilling results to serve as a reference for improving predictions and interpretations of future surveys in similar geologic settings.

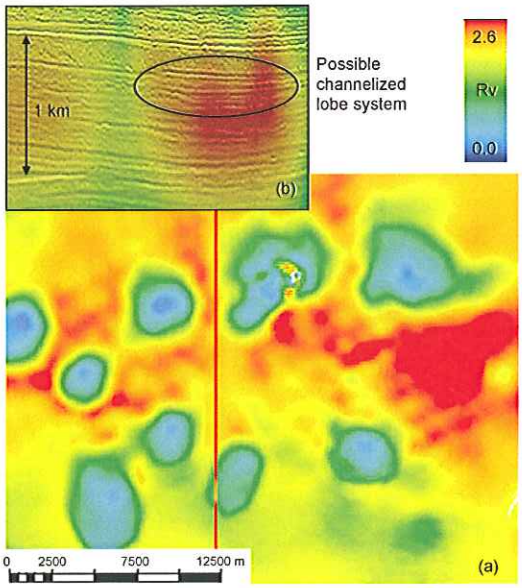

Figure 5: (a) Regional map of vertical resistivity; (b) co-visualization with seismic indicating a possible channelized lobe system.

DOI http://dx.doi.org/10.1190/segam2012-1181.1

http://dx.doi.org/10.1190/segam2012-1181.1

EDITED REFERENCES

Note: This reference list is a copy-edited version of the reference list submitted by the author. Reference lists for the 2012 SEG Technical Program Expanded Abstracts have been copy edited so that references provided with the online metadata for each paper will achieve a high degree of linking to cited sources that appear on the Web.

REFERENCES

Baltar, D., and Roth, F., 2012, Reserves estimation from 3D CSEM inversion for prospect risk analysis: Presented at the 74th Annual International Conference and Exhibition, EAGE.

Boswell, R., D. Shelander, M. Lee, T. Latham, T. Collett, G. Guerin, G. Moridis, M. Reagan, and D. Goldberg, 2009, Occurrence of gas hydrate in Oligocene Frio sand: Alaminos Canyon Block 818: Northern Gulf of Mexico: Marine and Petroleum Geology, **26**, no. 8, 1499–1512.

Buland, A., L. O. Løseth, A. Becht, M. Roudot, and T. Røsten, 2011, The value of CSEM data in exploration: First Break, **29**, no. 4, 69–76.

Ellingsrud, S., T. Eidesmo, S. Johansen, M. C. Sinha, L. M. MacGregor, and S. Constable, 2002, Remote sensing of hydrocarbon layers by seabed logging (SBL): Results from a cruise offshore Angola: The Leading Edge, **21**, 972–982.

Zach, J. J., A. K. Bjørke, T. Støren, and F. Maaø, 2008, 3D inversion of marine CSEM data using a fast finite-difference time-domain forward code and approximate hessian-based optimization: 78th Annual International Meeting, SEG, Expanded Abstracts, **27**, 614–618.

DOI http://dx.doi.org/10.1190/segam2012-1181.1